DOI: https://doi.org/10.14311/TPFM.2025.037

NUMERICAL STUDY OF CHARACTERISTICS AND CAVITATION PHENOMENA IN A CENTRIFUGAL PUMP IMPELLER

F. Yahi[1, 2], A. Meziane [3], Y. Hamnoune [2], N. Merabet[2], N. Azril [1], A. Talamali [1] and Abdelhalim Zemouri[1]

[1]Genie Physical of Hydrocarbons Laboratory, Faculty of hydrocarbons and chemistry, University M'Hamed Bougara, 35000 Boumerdes, Algeria.

[2]Thermodynamics and Energetic Systems Laboratory, Faculty of Physics, University of Sciences and Technology Houari Boumediene, B.P. 32 El Alia 16111 Bab Ezzouar, Algiers, Algeria.

[3]Fiabilité des équipements Pétroliers et Materieaux Laboratory, M'Hamed Bougara Boumerdes University, Algeria.

Abstract

This study focuses on the numerical analysis of characteristics and cavitation phenomena within centrifugal pumps, which are critical in various industrial applications. Firstly, we begin this investigation by analyzing the steady state to determine various characteristics of the centrifugal pump under study, including the head, net positive suction head, and the characteristic curve $H=f(Qv)$. Using ANSYS CFX, we tested three different meshes to obtain a solution that aligns well with the manufacturer's data (Nominal Flow Rate (Q), Head (H), Motor Power (P), Rotational Speed (rpm), Efficiency and $NPSH_{required}$ (required Net Positive Suction Head giving by the manufacturer)). Secondly, we proceed to study the cavitation phenomenon, which can dramatically affect pump performance and durability, leading to efficiency loss, noise, vibration, and structural damage. By considering an unsteady state regime and simulating different operating conditions, this research aims to understand the influence of key parameters, including impeller design and inlet pressure, on the intensity and location of cavitation. In our study, we focused on the variation of the inlet pressure (0.47 bar $\leq$ Pa $\leq$ 0.67 bar), which affects the NPSH (Net Positive Suction Head) and plays a significant role in the occurrence of cavitation. The results provide insights into minimizing cavitation effects, enhancing pump performance, and extending pump lifespan.

Keywords: Centrifugal pump impeller, CFD, Head, Power, Efficiency, Cavitation.

1 Introduction

Centrifugal pumps (Fig. 1), a subset of turbomachines, are widely used to transport liquids through piping systems. In operation, fluid enters the rotating impeller near its axis, where it gains velocity. The impeller directs the fluid radially outward into a diffuser or volute chamber, which then channels it into the downstream piping. These pumps are particularly effective for applications requiring high flow rates with relatively low pressure increases.

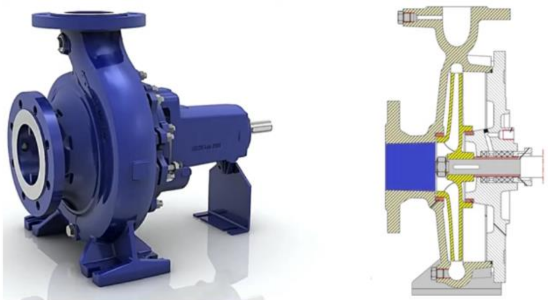

Figure 1: Centrifugal pump

Cavitation is a critical issue in the operation of centrifugal pumps, characterized by the rapid formation and collapse of vapor bubbles within the liquid being pumped. This phenomenon occurs when the local pressure in the pump falls below the liquid's vapor pressure, leading to vaporization. The subsequent implosion of these vapor bubbles generates shock waves that can cause significant damage to pump components, such as impellers, and result in decreased performance and efficiency.

Khin Cho Thin et al. [1] conducted a computational analysis of a centrifugal pump, predicting its performance at off-design flow rates and calculating various losses such as friction, slip, shock, and recirculation losses. E.C. Bcharoudis et al. [2] investigated the flow structures inside centrifugal impellers, noting a performance improvement of over 7% in head when the outlet blade angle was increased from 20° to 45°. Motohiko Nohmi et al. [3] developed cavitation CFD codes for centrifugal pumps and observed a breakdown in flow rate when cavities formed on both the suction and pressure surfaces. Vasilios A. et al. [4] optimized the blade inlet geometry for centrifugal pump impellers, while John S. Anagnostopoulos [5] developed an automated impeller design algorithm employing parametre optimization within the RANS solutions. M.H. Shojaee Fard and F.A. Boyaghchi [6] analyzed centrifugal pumps handling viscous fluids and found performance improvements with an increased outlet blade angle, which reduced wake formation at the impeller exit.

Recently, numerous numerical and experimental studies on cavitation phenomena in mixed-flow pumps have been published (e.g., [7-13]), though most primarily focus on steady cavitation. Kobayashi and Chiba [14] used Large Eddy Simulations (LES) to model unsteady hydraulic forces on the impeller of a mixed-flow pump under cavitation, while Yamamoto and Tsujimoto [15] conducted an extensive study on cavitation surge in centrifugal pumps. However, there is still a lack of detailed information in the literature regarding cavitation instabilities in mixed-flow or radial-flow pumps. Almost all studies on these instabilities focus on inducers, a specific type of axial-flow pump. Under cavitation conditions, inducers can experience a wide range of cavitation instabilities (Kamijo et al. [16], Tsujimoto et al. [17]), even at the design flow rate. Sedlar M. et al. [18] by using numerical modeling for cavitating flow in high-performance pumps used in power generation. They have highlighted three primary adverse effects of cavitation and analyzing them with practical examples. The numerical analysis combines the use of a commercial CFD code and in-house software that solves the Rayleigh–Plesset equation along flow paths. Additionally, cavitation bubbles are treated as active impurities that interact dynamically with the fluid during phase transitions, rather than being considered passive elements.

Understanding the mechanisms and effects of cavitation is essential for the design and maintenance of centrifugal pumps to ensure their reliability and longevity. This article delves into the causes, implications, and mitigation strategies related to cavitation in centrifugal pumps, providing insights to enhance operational performance and prevent potential failures.

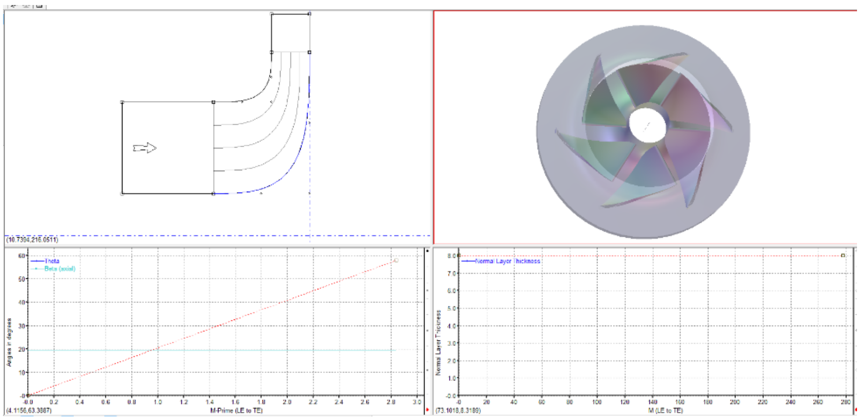

Figure 2: Impeller design

2 Centrifugal pump impeller designs

The design of the centrifugal pump focuses on the impeller part, which is carried out using the BladeGen module in ANSYS (Fig. 2). The operational parameters required for the pump are assumed to be as follows:

Table 1: Pump parameters

Head	Flow rate	RPM	Density
66.8m	1750m3/h	1500	10^3 Kg/ m^3

Input variables serve as a initial starting point for the pump design process. These variables, such as head, volumetric flow rate, rotational speed, and other key parameters, can be adjusted to meet the specific requirements of the intended application. The design interface provides multiple windows that display detailed information about the parameters, including the angular configuration of the blades, thickness distribution, and other geometric or performance-related attributes. This flexibility allows engineers to refine the design iteratively, ensuring optimal performance for a wide range of operating conditions.

3 Mesh generation

The computational mesh for the six-bladed pump impeller domain is created using ANSYS TurboGrid, a specialized tool for generating high-quality structured meshes for turbomachinery applications. To ensure adequate resolution and flexibility in modeling complex geometries, an unstructured mesh composed of tetrahedral cells is also employed for the impeller zones. This approach allows for precise capturing of the flow characteristics and geometric details. Resulting mesh distribution, illustrating the impeller and surrounding zones, is depicted in Figure 3. This combination of structured and unstructured mesh zones ensures a balance between computational efficiency and accuracy in representing the flow physics.

Table 2. Mesh Information

Nodes	Elements
1512840	1416355

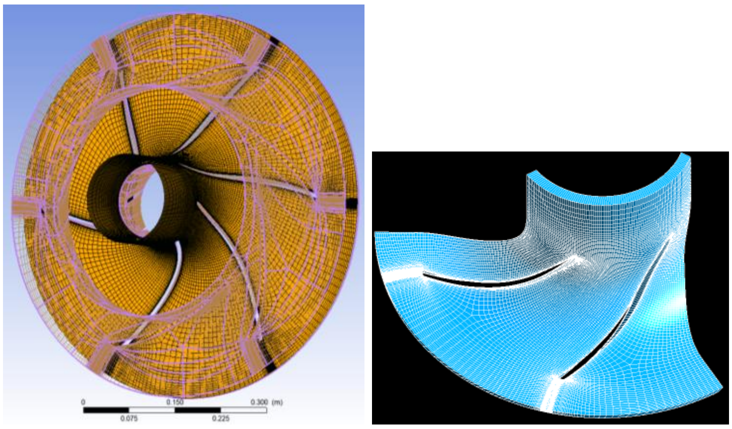

Figure 3: Impeller meshing

4. Boundary conditions

The centrifugal pump impeller domain is modeled as a rotating frame of reference, operating at a rotational speed of 1500 rpm. The working fluid within the pump is water at a temperature of 25°C, ensuring consistent thermophysical properties. To accurately capture turbulence effects, the widely-used k-ε turbulence model is employed for the steady state and k-Ω in the case of unsteady state, offering a reliable balance between computational efficiency and predictive accuracy for turbulent flows. Boundary conditions are defined with an inlet static pressure and an outlet mass flow rate of 444.44 kg/s, ensuring well-posed conditions for the simulation. The flow field is governed by the three-dimensional, incompressible Navier-Stokes equations, which are solved numerically using the ANSYS CFX Solver. This robust computational approach enables detailed analysis of the flow dynamics and performance characteristics of the pump under the specified operating conditions.

5. Results

The centrifugal pump impeller is analyzed at the design mass flow rate of **444.4 kg/s**. The performance results, including key metrics such as head and efficiency, are summarized in **Table 3**. Based on the Computational Fluid Dynamics (CFD) analysis, the head achieved by the pump is **119.425 m (mWG)**, while the total efficiency is determined to be $\eta = P_{hyd}/P_{total} = 76.82\%$. These results highlight the pump's ability to meet the specified design criteria under the given operating conditions. The analysis provides a comprehensive understanding of the pump's hydraulic performance, including flow distribution, pressure gradients, and energy conversion efficiency. Such insights are crucial for validating the design and identifying potential areas for optimization to further enhance performance.

Table 3: Performance parameters

Description	parameters	Units
Rotation Speed	**157.08**	radian/s
Reference Diameter	**0.4972**	m
Volume Flow Rate	**04479**	m^3/s
Head (LE-TE)	**135.629**	m
Head (IN-OUT)	**119.425**	m
Flow Coefficient	**0.0232**	
Head Coefficient (IN-OUT)	**0.192**	
Shaft Power	**677757**	W
Power Coefficient	**0.0058**	
Total Efficiency (IN-OUT) %	**77.1638**	
Static Efficiency (IN-OUT) %	**41.573**	

5.1 Pressure Contours on a meridional plane

In addition to analyzing the performance results of the centrifugal pump, the local characteristics of the internal flow field have been thoroughly examined. Pressure contours at 50% of the span and on meridional Surface locations, are illustrated in Figure 4.

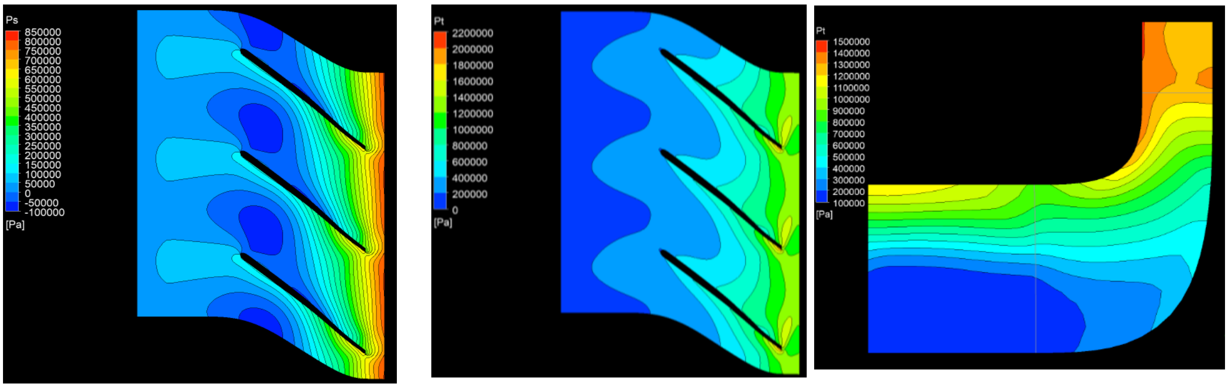

Figure 4: Contour of static and total pressure p_s, p_t at 50% of the span surface and on meridional

The pressure contours reveal a consistent increase in pressure from the leading edge to the trailing edge of the impeller, resulting from the dynamic head generated by the rotating impeller. It is noted that the total pressure on the pressure side of the blade is significantly higher than on the suction side. Furthermore, the pressure difference between the pressure side and the suction side of the impeller blade progressively increases from the leading edge to the trailing edge. The lowest value of static pressure within the impeller is observed at the leading edge of the blades on the suction side.

The total pressure distribution varies along the span of the impeller. Lower total pressures are observed near the hub of the impeller, while higher total pressures are recorded as the span increases, attributed to the greater dynamic head at the blade tip. Near the leading edge on the suction side of the blade, low total pressure and high velocity are observed, which can be linked to the thickness of the vane. At the trailing edge of the blade, total pressure losses occur across all span-wise locations due to wake formation in this region.

5.2 Blade loading at 20%; 50% and 80% span

The blade loading plot for the centrifugal impeller at 20%, 50%, and 80% span is illustrated in Figure 5. A steady increase in pressure is noted along the streamwise direction. High pressure is observed on the pressure side of the blade, while low pressure is present on the suction side. Near the leading edge, a pressure drop occurs on both the pressure and suction sides due to the acceleration of the flow into the impeller. At the trailing edge, a pressure drop is detected as a result of the blade wake.

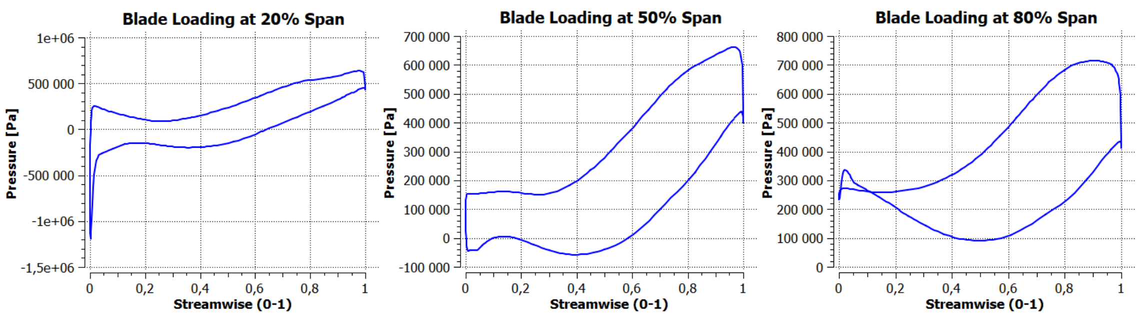

Figure 5: Blade Loading at 20%; 50% and 8% Span

Figures 6 illustrate the evolution of static and dynamic pressures within the pump. It is observed that the pressures remain constant near the inlet and begin to increase from position 0.4, reaching their maximum at the blade outlet with a value of 12 bars for 80% of the total blade height. This increase is due to the variation in dynamic pressure, which is given by the equation: $\boldsymbol{p_{dyn}=1/2\rho U^2}$. It is also noted that the total pressure is higher than the static pressure throughout the blade passage, which is explained by the relation $\boldsymbol{p_t = p_s+p_{dyn}}$.

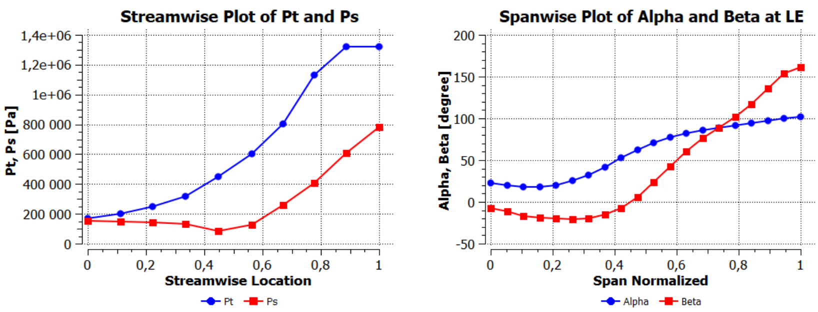

Figure 6: Streamwise Plot of Pt and Ps

5.3 Streamwise variation of relative and circumferential velocity

Figure 7 presents the evolution of the relative and circumferential velocity versus streamwise location. It is noted that, starting from the blade inlet (region where the fluid first comes into contact with the blade), the circumferential velocity tends to gradually increase, reaching a maximum velocity at the leading and trailing edges of 38 m/s (maximum velocity provided by the supplier = 39.1 m/s). Afterward, the velocity decreases as it moves toward the blade outlet (region or point where the fluid leaves the surface of the blade). It is observed that from the blade inlet, the relative velocity tends to decrease, then slightly increases starting from point 0.4, and decreases again up to point 0.8, reaching a minimum velocity between 7 and 8 m/s. Subsequently, the velocity increases exponentially toward the impeller outlet, reaching a value of 17 m/s (the range provided by the supplier is between 16 and 19 m/s).

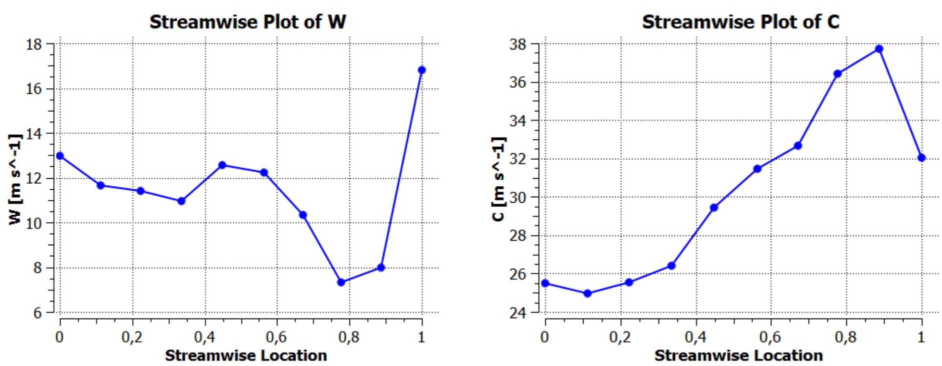

Figure 7: Streamwise plot of W and C velocities

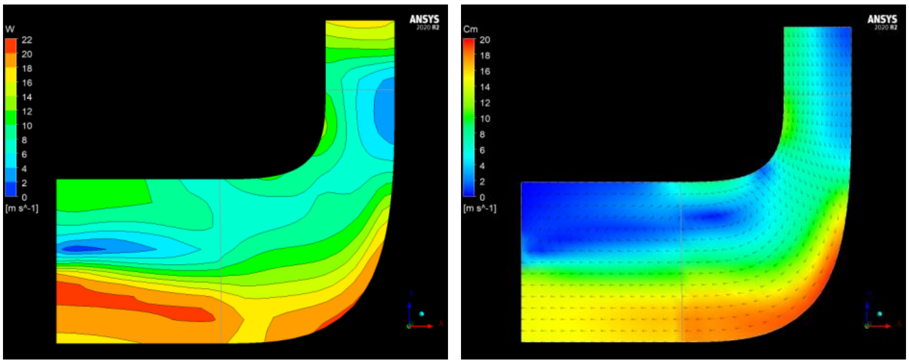

Figure 8: Contour of Mass Averaged W and Cm on Meridional Surface

5.4. Cavitation analysis

In practice, various criteria are used to determine the onset of cavitation. These criteria are typically based either on the static pressure, which must fall below the saturated vapor pressure over a specified minimum area, or on the calculated void fraction. In our analysis, we adopted the first criterion, which involves the static pressure approach. Specifically, we required the Net Positive Suction Head required NPSHreq to be reached, regardless of the area where this occurs. This method focuses on the pressure conditions necessary to prevent cavitation, ensuring that the pump operates within safe limits. By using the NPSHreq_criterion, we align with industry standards, providing a clear and measurable parameter to assess and control cavitation risks in various operating conditions.

Table 4: Pressure inlet corresponding to the Available NPSH

Pa (bar)	**0.67**	**0.65**	**0.63**	**0.61**	**0.59**	**0.57**	**0.55**	**0.53**	**0.51**	**0.49**	**0.47**
NPSH (m)	**6.3**	**6.1**	**5.9**	**5.7**	**5.5**	**5.3**	**5.1**	**4.9**	**4.7**	**4.5**	**4.3**

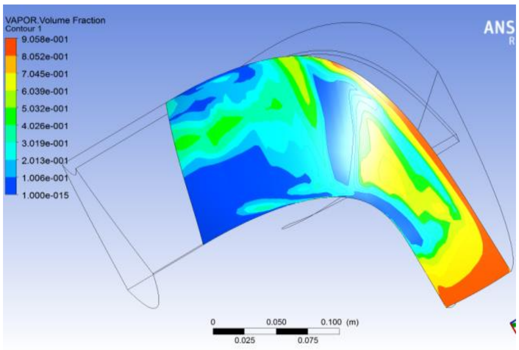

(a) P=0.47 bar

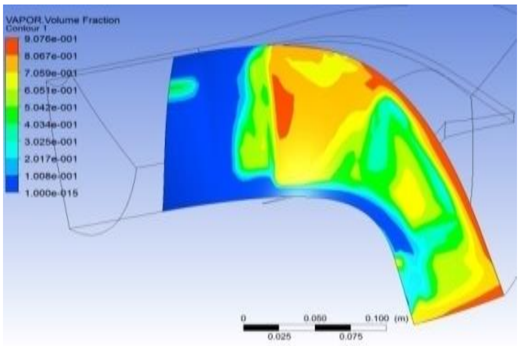

(b) P=0.57bar

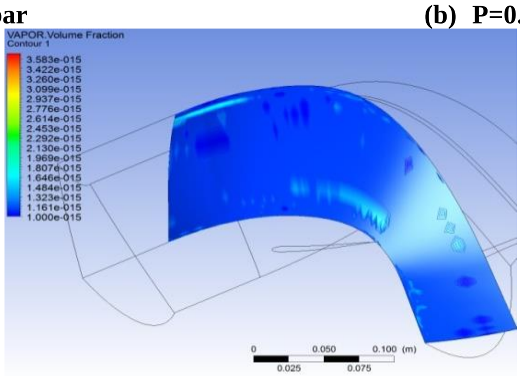

(c) P=0.67 bar

Figure 9: Volume fraction of water vapor at T=25°C

Figure 9 (a) shows a high vapor volume fraction near the blade's trailing edge. The gradient of colors from blue (low vapor) to red (high vapor) indicates significant cavitation occurring at this region. This suggests a local pressure drop below the vapor pressure. In Figure 9 (b) cavitation is less pronounced compared to the first figure. The vapor is concentrated near the blade's leading edge, showing a shift in cavitation onset due to possible changes in flow conditions or geometry. The vapor volume fraction is minimal or almost nonexistent throughout the blade passage, with most of the region in blue. This indicates an absence of cavitation, suggesting improved pressure conditions or a higher NPSH available Figure 9 (c). On the Leading and trailing edge, the velocity is maximum and gradually increases towards the exit of the blade - Figure 10 (a-c).

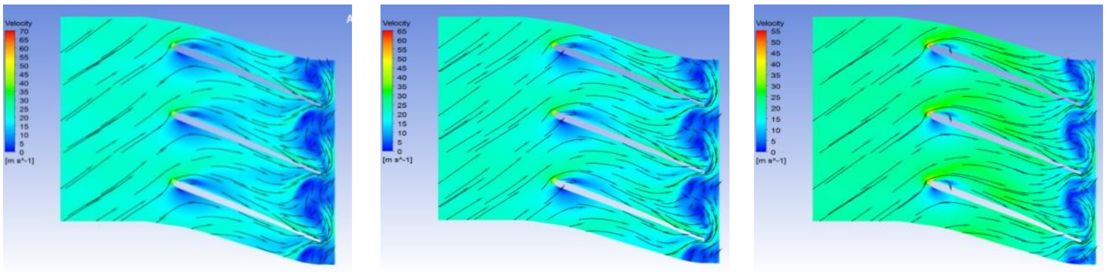

(a) P=0.47bar **(b) P=0.57 bar** **(c) P=0.67 bar**

Figure 10: Contour of Velocity at 50% span

6. Conclusion

A centrifugal pump impeller is modeled and analyzed using computational fluid dynamics (CFD) to simulate the flow of fluid, predict performance characteristics, and optimize design parameters. The CFD simulation allows for detailed examination of velocity distribution, pressure profiles, and turbulence behavior within the impeller, offering valuable insights into pump efficiency, cavitation potential, and operational stability under various conditions. This computational approach enables the identification of design improvements and performance enhancements that may not be easily observed through experimental methods alone.

After performing mesh testing, we identified the appropriate mesh that provided the most optimal values for various parameters, such as the outlet pressure. These results perfectly match the information provided by the manufacturer. Additionally, a transient simulation was conducted to study the cavitation phenomenon. From the simulations, it can be concluded that the discretization of the part (mesh) is the most crucial step in the simulation process. It is the step that ensures results closer to those of the manufacturer, provided it is correctly mastered.

References

[1] Khin C. T., Mya M. K. & Khin M. A.: Design and Performance Analysis of Centrifugal Pump. *World Academy of Science, Engineering and Technology*: (2008) pp 46.

[2] Bcharoudis E.C., ilios A.E., Mentzos M.D. & Margaris D.P.: Parametric Study of a Centrifugal Pump Impeller by Varying the Outlet Blade Angle, *The open Mechanical Engineering Journal*, (2008) pp75-83.

[3] Motohiko N., Akira G.: Cavitation CFD in a Centrifugal pump, *Fifth international symposium on cavitations,* Osaka, Japan, November 2003.

[4] Grapsas V. A., Anagnostopoulos J. S. & Papantonis D. E.: Hydrodynamic Design of Radial Flow Pump Impeller by Surface Parameterization, *International Conference on Experiments / Process / System Modeling / Simulation / Optimization,* Athens, 6-9 July, 2005.

[5] Shojaee M.H. Fard & Boyaghchi F.A.: Studies on the influence of various blade outlet angles in a centrifugal pump when handling viscous fluids, *American Journal of Applied Sciences*, (2007) pp.718-724.

[6] Anagnostopoulos J. S.: CFD Analysis and Design Effects in a Radial Pump Impeller, *Wseas Transactions on Fluid Mechanics,* (July 2006) Vol 1.

[7] Os M.J., Op de Woerd J.G.H & Jonker, J.B.: A Parametric Study of the Cavitation Inception Behaviour of a Mixed-Flow Pump Impeller Using a Three-Dimensional Potential Flow Model, (1997), *Proc. ASME FEDSM97*-3374.

[8] Nagahara, T., Sato, T and Okamura, T.: Effect of the Submersed Vortex Cavitation Occurred in Pump Suction Intake on Hydraulic Forces of Mixed Flow Pump Impeller. *CAV2001:sessionB8.006,* (2001), pp. 1-8.

[9] Sedlar, M.: Numerical Investigation of Flow in Mixed-Flow Pump with Volute. TASK QUARTERLY *5,* (2001), No. 4, pp. 595-602.

[10] Sedlar, M., Marsik, F. and Safarik, P.: Numerical Analysis of Cavitated Flows in Mixed-Flow Pump Impellers. *Proc. Proc 3rd Int. Conference on Transport Phenomena in Multiphase Systems, Heat* (2002), pp. 461-466.

[11] Sedlar, M., Zima, P. and Muller, M.: CFD Analysis of Cavitation Erosion Potential in Hydraulic Machinery. *Proc. 3rd IAHR WG Meeting* (2009), pp. 205-214.

[12] Oh, H.W.: Design Parameter to Improve the Suction Performance of Mixed-Flow Pump Impeller. *Proc. IMechE Vol. 224, Part A: J. Power and Energy, JPE986,* (2010), pp. 881-887.

[13] Harada, I., Kobayashi, K. & Ono, S.: Prediction of Axial Thrust for Mixed-Flow Pumps with Vaned Diffuser by Using CFD. *Int. Journal of Fluid Machinery and Systems,* (2010) Vol. 3, No. 2, pp. 160-168.

[14] Kobayashi, K. & Chiba, Y.: Computational Fluid Dynamics of Cavitating Flow in Mixed Flow Pump with Closed Type Impeller. *Int. Journal of Fluid Machinery and Systems.* (2010) Vol. 3, No. 2, pp. 113-121.

[15] Yamamoto, K. & Tsujimoto, Y.: Backflow Vortex Cavitation and Its Effects on Cavitation Instabilities. *Int. Journal of Fluid Machinery and Systems,* (2009) Vol. 2, No. 1, pp. 40-54.

[16] Kamijo, K., Shimura, T. & Watanabe, M.: An Experimental Investigation of Cavitating Inducer Instability. *ASME* (1977), Paper 77-WA/FW-14.

[17] Tsujimoto, Y., Yoshida Y., Maekawa M., Watanabe S. & Hashimoto T.: Observations of Oscillating Cavitation of an Inducer. *ASME Jour. Fluids Engng.* (1997) 119, No. 4, pp. 775-781.

[18] Sedlar M., Šoukal J., Krátký T., Vyroubal M.: prediction of impacts of cavitation in pumps for power generation. *Thermal Engineering,* (2015), Vol. 62, No. 6, pp. 408–413.